Conservation of Cultural Stones: Relationship Among Texture, Thermal Ageing and Consolidation Strategies in White Apuan Marbles

Marco Lezzerini*, Simona Raneri, Marco Nutarelli and Letizia Luti

Department of Earth Sciences - University of Pisa, Via S. Maria 53, 56126, Pisa, Italy

Abstract: A major problem in the conservation of stone materials concerns durability and the use of compatible and efficacy conservation treatments. Among cultural stones, white Apuan marble stands out for its wide diffusion in built environment; thus, the study of its decay and the recognition of smart solution for its conservation is a quite relevant issue. In spite of an aesthetical homogeneity, white marbles exhibit a range of textural features able to influence their durability. The aims of this study are therefore to evidence the relationship between decay and textural features in marbles, and to test the efficacy of some innovative nanostructured products in comparison to ethyl-silicate. Ten white marbles from different Apuan Alps quarrying areas, characterized by a range of textural features, were analyzed. Preliminary, textural, mineralogical and chemical analysis have been performed by petrographic, XRD, and XRF analyses; physical properties were determined by both capillarity and water absorption by total immersion tests on specimens. After an initial drying at 60±5°C, specimens were artificially aged by thermal stresses (cycles at 110°C, 110°C and cooling in water, 250°C, and 550°C). The comparison of physical parameters before and after thermal stresses allows evaluating the influence of some textural factors (especially grain boundaries and mean grain size) on the decay. Artificially thermal damaged samples were subsequently treated with two nanostructured products, nano-lime and nano-silica, and with ethyl-silicate, to compare the efficacy of innovative consolidants in respect to a traditional one. The efficacy was evaluated on the basis of water absorption behavior of marbles before and after treatments. The study evidenced better performances of nano-silica in respect to nano-lime, even ethyl-silicate confirmed its high effectiveness in consolidating marbles regardless their textural features.

Keywords: Marbles, Thermal damage, Decay, Consolidant, Nano-materials.

1. INTRODUCTION

White Apuan marble is one of the most used cultural stone worldwide, both in ancient and modern masonry; for this reason, the inspection of problems related to decay and conservation are of great interest in Cultural Heritage and Engineering Sciences. In spite of an aesthetical, chemical and mineralogical homogeneity, marbles quarried from Apuan Alps basins exhibit a quite relevant variability in term of textural and structural features [1], due to different tectonic events that involved Apuan complex [2]. Numerous studies [3-8] have evidenced that such a diversity has a key role in hydric behavior of marbles, determining a diverse response to decay processes. In particular, grain boundaries seem to have a relevant role in cracks opening and propagation, while grain size seems to have lower importance [9].

The detailed knowledge of marble response to decay is fundamental to plan smart conservative strategies, especially regarding stone consolidation. Among the main requirements of a consolidant, physical and chemical compatibility, stability, reversibility, and appropriate penetration depth are especially demanded [10]. In the last decade, the synthesis and application of innovative products able to improve long-term stone conservation has greatly increased [11]. In this context, a particular attention has been devoted to nanomaterials [12-15], making it possible to obtain highly efficient products able to penetrate even in small pore structures. Of course, the use of innovative consolidants and coatings into Cultural Heritage monuments requires a preliminary laboratory testing to evaluate their effectiveness, compatibility and durability, as well as their ability to penetrate into pore structure of the stones; this latter aspect is particularly relevant for marbles, due to their low porosity.

The present work intends therefore to improve knowledge on decay and conservation of marbles, by providing insights about the possible relationship between textural features and decay due to artificial thermal damage and the performances of nanostructured consolidants, based on nano-lime and nano-silica particles.

*Address correspondence to this author at the Department of Earth Sciences - University of Pisa, Via S. Maria 53, 56126, Pisa, Italy; E-mail: marco.lezzerini@unipi.it

E-ISSN: 2414-2115/17

2. MATERIALS AND METHODS

2.1. Selected Marbles

Ten different white marbles from quarrying areas representative of the variability of the Apuan Alps basins were selected (Figure **1**) for this study.

In detail, six set of samples from Colonnata basin (labeled as OL, GR, CO, P2, PET and GI), three from Miseglia-Fantiscritti basin (labeled as TO, CG and FS), and one from Torano basin (labeled as LF) were taken from quarries exploited over the time to supply cultural stones.

2.2. Characterization of Marbles

2.2.1. Petrographic, Mineralogical and Chemical Analyses

The main textural features of studied marbles (*i.e.:* shape, dimension and orientation of crystals, boundaries, etc.) were inspected by both optical microscope and image analysis on thin sections. Average values of area, perimeter, long and short axes length, and long axis orientation were determined on less than 200 grains for each sample. According to [16], the following parameters were calculated: average diameter (D), equivalent diameter (D_{eq}), form factor (F), sphericity (S), elongation (E).

Qualitative mineralogical analysis were performed by an X-ray diffractometer Philips PW 1730 (XRD), equipped with a X-ray tube with copper anode ($Cu_{K\alpha}$ radiation) and nickel (Ni) filter for the suppression of the K_β of the incident radiation. Randomly oriented powders (both of bulk and insoluble residue) have been scanned from 4 to 60 °2θ, with 1° 2θ step size, counting time of four seconds per step, and voltage and current of 36 kV and 24 mA, respectively.

X-ray fluorescence analysis (XRF) were also carried out to obtain the chemical composition of the samples.

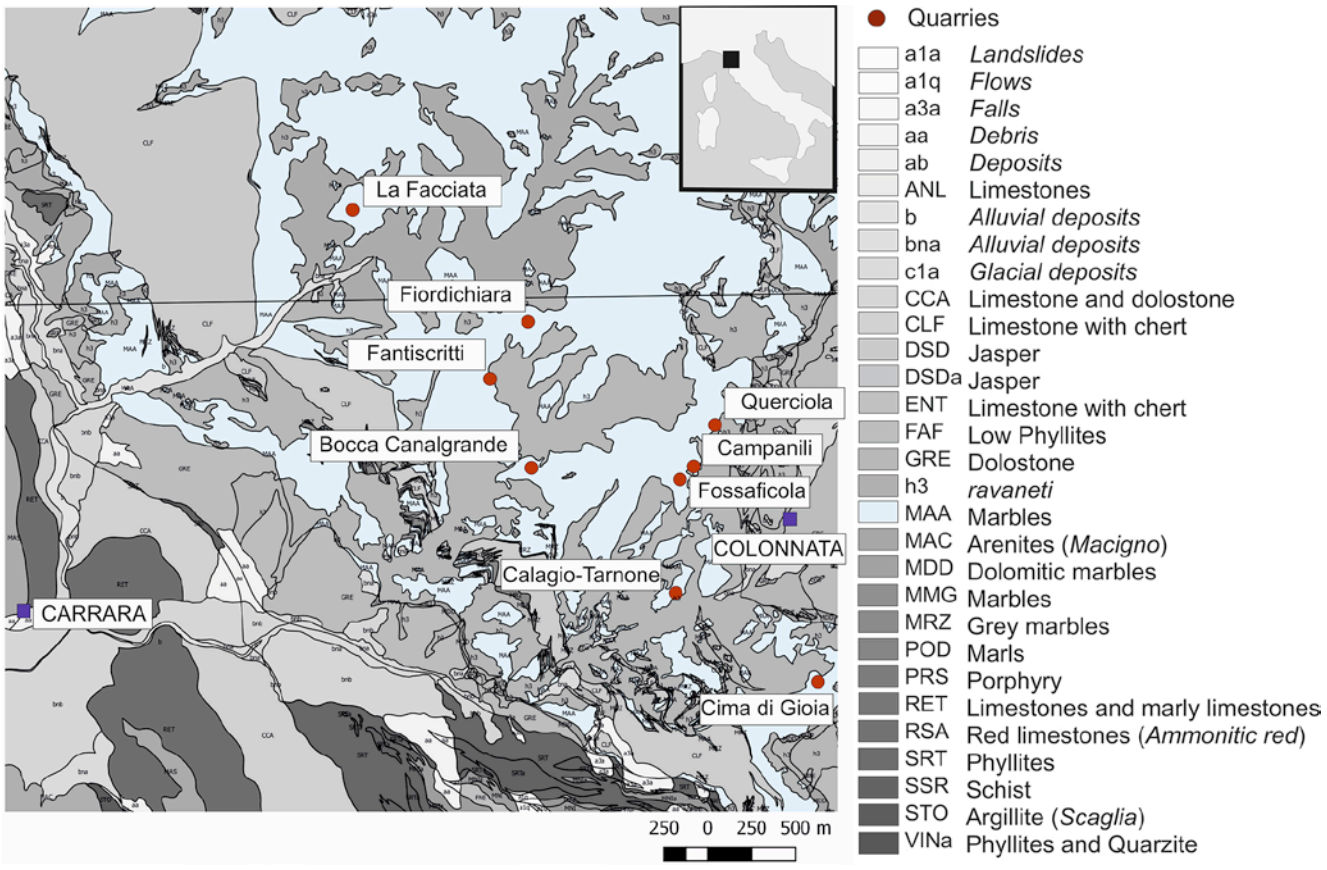

Figure 1: Geological sketch map of Apuan Alps with indications on sampling sites within Colonnata, Miseglia-Fantiscritti and Torano basins (modified by http://www502.regione.toscana.it/geoscopio/geologia.html#). Localities: Calagio-Tarnone, Colonnata basin (Carrara), sample OL; Campanili (NW Colonnata centre), Colonnata basin (Carrara), samples GR and PET; Fossaficola (Campanili), Colonnata basin (Carrara) sample CO; Querciola, Colonnata basin, sample P2; Cima di Gioia, Colonnata basin, sample GI; Fiordichiara (Miseglia), Miseglia-Fantiscritti basin (Carrara), sample CG; Bocca Canalgrande (Miseglia), Miseglia-Fantiscritti basin (Carrara), sample FS; Fantiscritti, Miseglia-Fantiscritti basin, sample TO; La Facciata (Torano), Torano basin, sample LF.

Major elements (Na_2O, MgO, Al_2O_3, SiO_2, P_2O_5, K_2O, CaO, TiO_2, MnO, Fe_2O_3) were determined on pressed powder pellets by an ARL 9400 XP+ sequential X-ray spectrometer under the instrumental conditions reported in [17]. Within the range of the measured concentrations, the analytical uncertainties are <5% for all the components except for Na_2O, P_2O_5, TiO_2 and MnO which may occasionally attain <10% for very low concentrations [17-18].

The amount of the volatile components was determined as loss on ignition (LOI in 105-950°C temperature range). The CO_2 content was also measured by using the calcimetry method [19] on 300 mg of finely powdered samples previously dried at 105±5°C.

2.2.2. Physical Tests

For each marble sample, real (G) and apparent (γ_d) densities, and total porosity (P%) were calculated assuming values of 2.711 g/cm^3, 3.037 g/cm^3, 2.872 g/cm^3, 2.653 g/cm^3 for calcite, magnesite, dolomite and quartz, respectively [20]. The physical properties values were calculate according to the following formulas:

$$G = \sum_i x_i G_i \ [\frac{\mathrm{g}}{\mathrm{cm}^3}] \ , \tag{1.1}$$

with x_i and G_i weight and real density of i-th component;

$$\gamma_d = \frac{m}{V_a} \ [\frac{\mathrm{g}}{\mathrm{cm}^3}] \ , \tag{1.2}$$

with m and V_a mass and apparent volume of specimens, the latter obtained by hydrostatic balance method [21];

$$P = \left(1 - \frac{\gamma_d}{G}\right) \cdot 100 \ [\%] \tag{1.3}$$

with G and γ_d real density and apparent density, respectively.

The mass of absorbed water by capillarity was determined according to UNI EN 15801:2010 [22]. Cubic samples were placed in a vessel on a blotting paper stratum saturated with demineralized water and weighted at 6, 10, 20, 30, 45 min, 1, 2, 3, 4, 5, 6, 7, 8, 24, 48 and 72 h. The amount of water absorbed Q_i (mg cm^{-2}) at time t_i was calculated by

$$Q_i = \frac{M_i - M_0}{A} \ , \tag{1.4}$$

where M_0 is the mass of the dry specimen (mg), M_i is the mass (mg) at time t_i, and A is the area in contact with the wet paper (cm^2).

The calculated values of Q_i were reported as function of the square root of time ($t_i^{0.5}$). The absorption coefficient AC (mg cm^{-2} s$^{-0.5}$) was calculated as the slope of this curve at the beginning of the test (t_i < 30 min), when the amount of water absorbed Q_i as function of $t^{0.5}$ is approximately linear.

At the end of the test, samples were immersed in water and weighted each 24^h until constant mass to determine the water absorption by total immersion

$$IC_w = \frac{M_w - M_0}{M_0} \cdot 100 \ [\%] \tag{1.5}$$

with M_w and M_0 wet and dry mass, respectively.

Water absorption IC_v, expressed in volume, was calculated by:

$$IC_v = \frac{M_w - M_0}{V_a} \cdot 100 \ [\%] \tag{1.6}$$

Water saturation index (SI) was calculated by:

$$SI = \frac{IC_v}{P} \cdot 100 \ [\%] \tag{1.7}$$

2.3. Thermal Stress

Accelerating ageing tests were performed by thermal stresses [23] on four sets, consisting in three cubes for each marble variety, by repeating the following cycles: (i) 20 cycles at 105±5°C and cooling at room temperature; (ii) 20 cycles at 105±5°C and cooling in water (according to UNI EN 14066:2013 [24]); (iii) 1 cycle at 250±5°C and cooling at room temperature; (iv) 1 cycle at 550±5°C and cooling at room temperature. At the end of the thermal cycles, water absorption tests were repeated to evaluate possible changes in the hydric behavior of marble due to thermal damage.

2.4. Treatments of Marbles and Efficacy Tests

Artificially damaged stone samples were treated with three commercially available consolidants to evaluate the efficacy of innovative and nano-sized products, nano-lime and nano-silica, in comparison with a classical product employed in marble consolidation, ethyl-silicate.

In detail, the treatments includes: (a) Albi 700 (EtOH), ethyl-silicate diluted in isopropanol (30%); (b) Nanorestore (nano-lime), consisting in $Ca(OH)_2$ nanoparticles (40-200 nm in dimension) dispersed in isopropyl alcohol (99.5%); (c) NanoEstel (nano-silica), consisting in silica nanoparticles (10-20 nm in dimension) dispersed in water (70%).

Cubes were plunged into products in sealed containers for 8 h and dried at room temperature for 10 days, to assure the reticulation of the products. Water absorption tests were repeated on treated samples, in order to evaluate the efficacy of the products. Capillarity index, water absorption by total immersion, saturation index and porosity were therefore calculated and compared with the values obtained on untreated damaged samples.

3. RESULTS AND DISCUSSION

3.1. Marble Characterization

Table **1** shows the chemical composition of major elements obtained by XRF analysis. The composition of analyzed marble is mainly due to CaO, which levels range from 54.23 (in sample GI) to 54.99 wt.% (in sample TO). Small amount of MgO (from 0.63 in FS and TO to 1.17 % in GI) and other components (< 0.45±0.15%), related to the presence of dolomite, albite, quartz, pyrite and muscovite (detected by XRD analysis as listed in Table **2**) are also present.

Data obtained by image analysis are reported in Table **3**, while in Figure **2** micro-textural features of the three main fabrics observed in this study are shown.

Table 1: Chemical Composition Determined by XRF, Expressed as Weight Percentage

Sample ID	*P.C.*	*Na_2O*	*MgO*	*Al_2O_3*	*SiO_2*	*P_2O_5*	*K_2O*	*CaO*	*TiO_2*	*MnO*	*Fe_2O_3*
OL	43.94	< 0.01	0.77	0.04	0.08	0.23	< 0.01	54.92	< 0.01	0.01	0.01
GR	43.97	< 0.01	0.91	0.03	0.09	0.21	0.01	54.77	< 0.01	< 0.01	0.01
CO	43.97	< 0.01	0.99	0.07	0.12	0.15	0.01	54.66	< 0.01	0.01	0.02
P2	43.92	< 0.01	0.80	0.07	0.15	0.19	0.01	54.84	< 0.01	< 0.01	0.02
PET	44.02	0.07	1.11	0.07	0.15	< 0.01	0.02	54.54	< 0.01	< 0.01	0.02
GI	43.85	< 0.01	1.17	0.06	0.39	0.25	0.01	54.23	< 0.01	0.01	0.03
CG	44.00	0.02	0.84	0.05	0.12	0.04	0.01	54.90	< 0.01	< 0.01	0.02
FS	43.81	< 0.01	0.63	0.06	0.25	0.26	0.01	54.96	< 0.01	0.01	0.01
TO	43.84	< 0.01	0.63	0.06	0.14	0.30	0.01	54.99	< 0.01	0.01	0.02
LF	43.91	< 0.01	0.76	0.05	0.09	0.27	< 0.01	54.90	< 0.01	0.01	0.01

Table 2: Qualitative Mineralogical Composition of Insoluble Residue to Dilute Acid Attack

Sample ID	*Albite*	*Quartz*	*Dolomite*	*Pyrite*	*Muscovite*
OL	X		x	x*	x
GR				x	x
CO	X		x	x	x
P2		x	x	x	x
PET	X	x	x	x*	x
GI		x		x*	x
CG	X	x	x	x	x
FS	X	x		x*	x
TO	X	x	x	x	x
LF	x	x		x	x

The symbol * marks phases identified by thin section analysis.

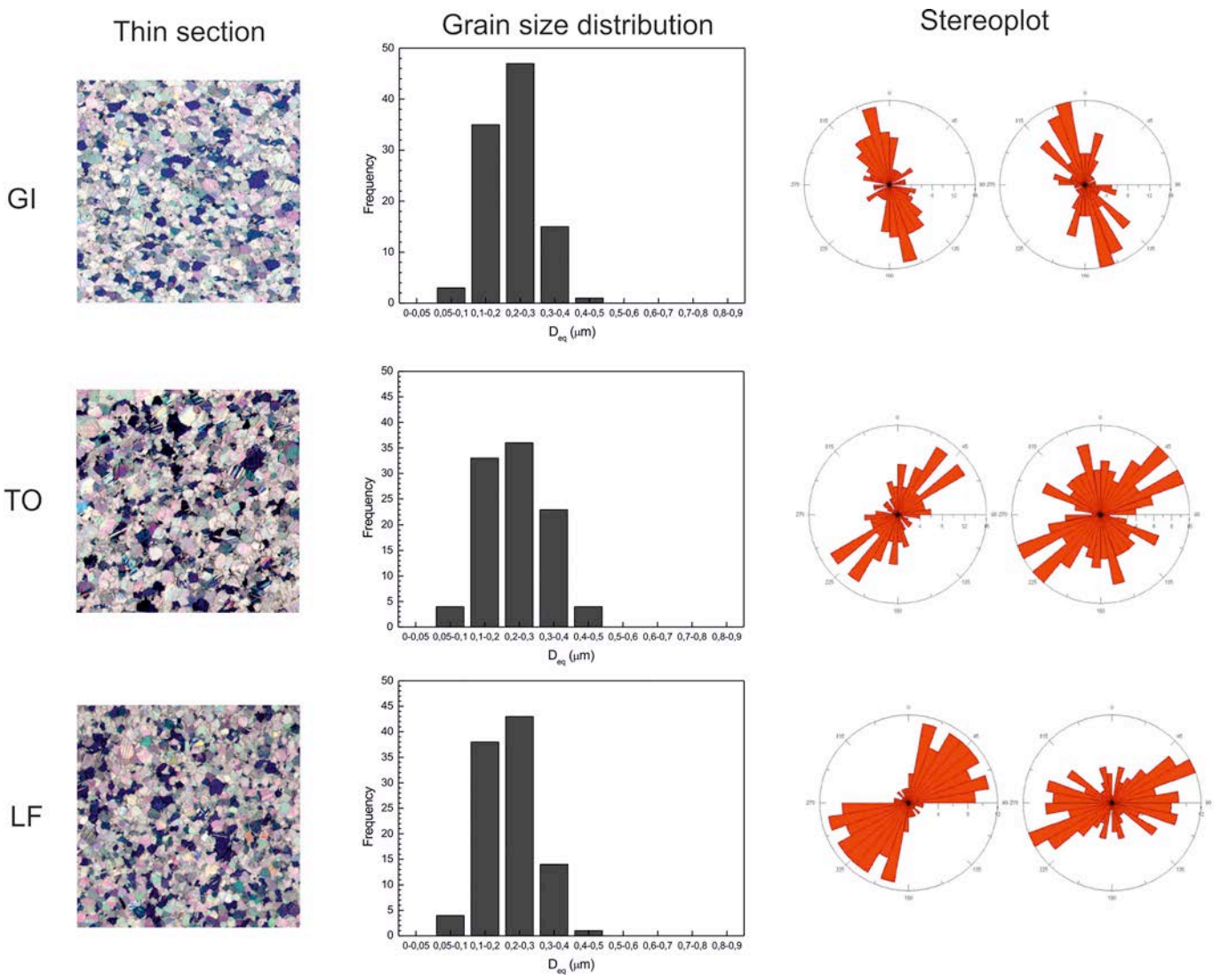

Figure 2: Textural features of some studied marbles, representative of the different fabric identified.

Overall, the studied marbles exhibit etheroblastic texture, with the exception of P2 (Querciola, Carrara basin) and LF (La Facciata, Torano basin) samples, for which xenoblastic texture was observed. Grain size ranges from medium to low, with D_{eq}> 250 μm in FS (Miseglia-Fanscritti) and OL (Carrara), $D_{eq} \cong$ 250 μm in GI and GR (Carrara), and TO (Miseglia-Fanscritti) samples, D_{eq}<250 μm in CG (Miseglia-Fanscritti), CO, P2, PET (Carrara), LF (Torano). Grain boundaries are mainly straight in FS, GI e GR, from curved to straight in CG, CO, OL, PET and TO, and from lobates to curved in LF and P2 samples.

In Table **4**, physical parameters along with porosity, saturation index and water absorption calculated from total water immersion and capillarity tests are reported. The inspection of the obtained data clearly suggests a dependence of physical properties on textural features of studied marbles (Figure **3**).

In particular, an increasing of water absorption (by both capillarity and total immersion) for marbles with increasing equivalent diameter can be observed; otherwise, inverse proportionality between grain size and apparent density can be assessed. Specifically, samples with average grain size <250 μm show the lowest values of the measured parameters. Additionally, grain boundaries seem to have an influence on hydric proprieties of the studied materials; regardless grain size, marbles with lobates boundaries (LF and P2 samples) show lower porosity values and absorb less water than marbles with straight and curves boundaries.

3.2. Textural and Physical Properties vs. Thermal Ageing

The already evidenced textural differences affect not only the water absorption behavior of studied marbles, but also the extent of decay. In fact, the

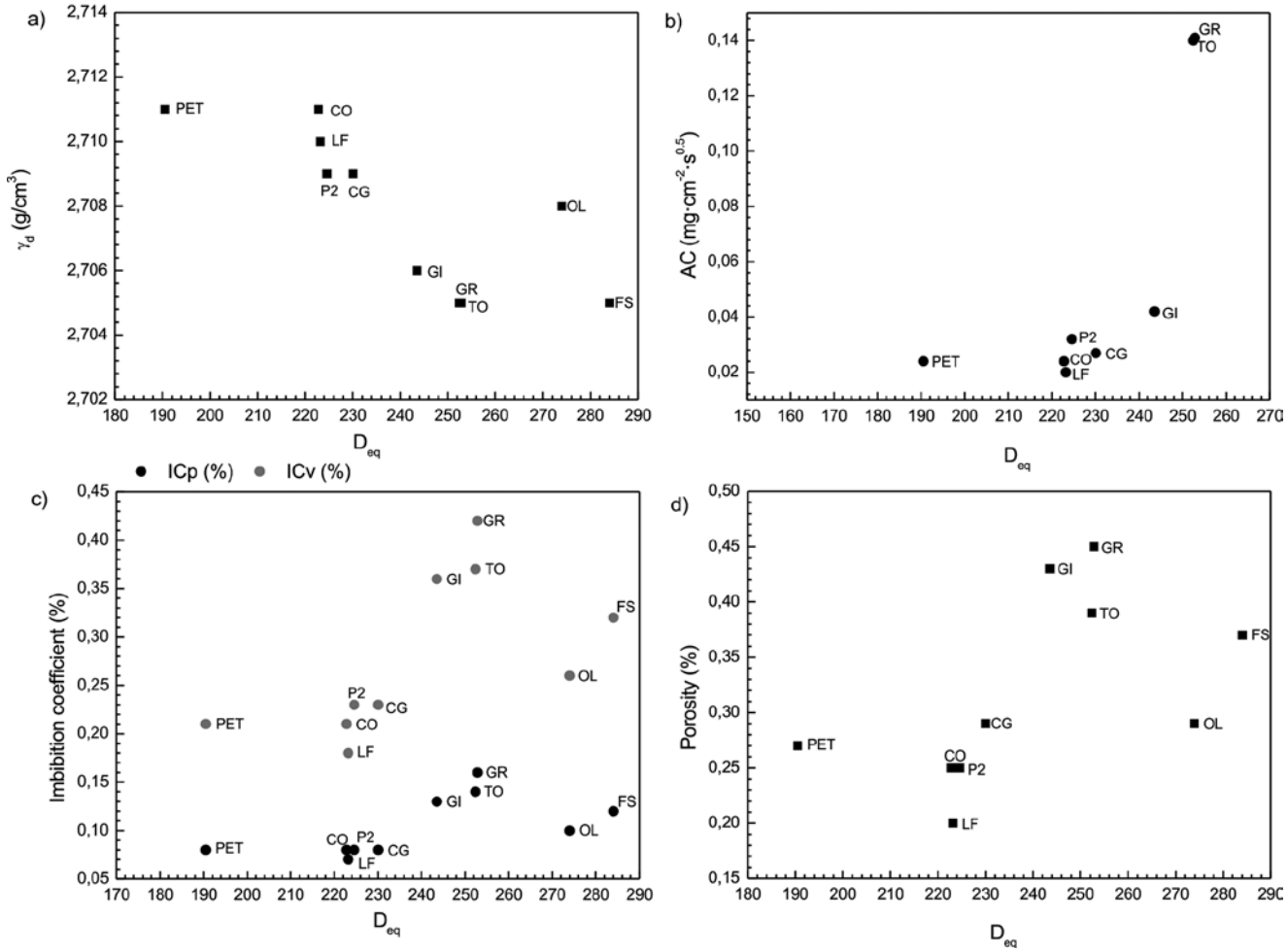

Figure 3: Variation of physical parameters in function of grain size of studied marble (expressed as D_{eq}).

accelerated damage by thermal stress contributes to empathize the different behavior of marbles exhibiting various grain boundaries and grain size.

Overall, artificially damaged marbles absorb more water (by both capillarity and total immersion) than un-weathered ones (Figure **4**), even at low temperature stress. A significant increase of capillary absorption coefficient, water absorption by total immersion, porosity and saturation index values (Table **5** and Table **6**) is evident after thermal cycles at temperatures above 250°C (Figure **5** and Figure **6**). Moreover, the cooling in water seems to have a great influence in thermal damage [25]: samples artificially damaged by 20 cycles at 105±5°C and cooled in water suffer a higher increase of water absorption by capillarity than samples degraded at 250±5°C and cooled at room temperature (see Figure **4**). This behavior is especially evident for CG, CO, LF, P2 and PET marbles.

Going to relations between thermal damage and textural features, noteworthy is that the greater variation of the measured parameters have been collected on samples exhibiting straight boundaries (from Carrara and Miseglia-Fantiscritti basins) (see Table **6**).

3.3. Efficacy of Tested Consolidant Products

The average variations in absorption parameters due to the applied treatment are reported in Table **7**, while in Figure **7** water absorption curves acquired on treated samples artificially damaged by 20 cycles at 105±5°C and cooled in water are shown, as example.

The obtained results clearly show that ethyl-silicate greatly slows down the water absorption ability of studied marbles, regardless grain size and porosity (even when the latter one is significantly increased by thermal stresses). Otherwise, nano-particle based consolidants seem to be less efficient, even if nano-silica treatment assures a relevant reduction of water absorption.

The inspection of values reported in Table **7** allows evaluating the ability of the products to interact with the

Table 3: Main Textural Parameters of Studied Marbles

Basin	Localization	Sample ID	Texture	Boundaries	Min (μm)	Max (μm)	MGS (μm)	P (μm)	A (μm^2)	D_{eq} (μm)	D (μm)	F	S	E
Carrara	Calagio-Tarnone	OL	granoblastic-eteroblastic	from curved to straight	232±85	325±117	720	1001±374	0.066±0.045	274±97	279±98	753±79	847±74	723±121
	Campanili	GR	granoblastic-eteroblastic	mainly straight (rare curved)	214±69	294±90	600	906±287	0.054±0.032	253±76	257±77	761±65	855±70	735±118
	Fossaficola	CO	granoblastic-eteroblastic	from curved to straight	185±69	264±96	620	809±313	0.043±0.032	223±79	228±80	749±77	839±85	711±139
	Querciola	P2	from xenoblasic to granoblastic-eteroblastic	from lobates to curved	189±76	270±104	640	818±327	0.046±0.035	225±87	229±88	763±76	839±76	710±122
	Campanili	PET	granoblastic-eteroblastic	from curved to straight	160±61	228±88	580	685±275	0.032±0.025	191±71	195±73	774±75	840±83	712±136
	Cima di Gioia	GI	granoblastic-eteroblastic	mainly straight (rare curved)	208±73	289±103	730	881±327	0.053±0.035	244±84	248±85	768±68	851±72	729±120
Miseglia-Fantiscritti	Fiordichiara	CG	granoblastic-eteroblastic	from curved to straight	192±77	278±108	660	850±356	0.048±0.038	230±88	235±90	747±85	834±75	699±123
	Bocca Canalgrande	FS	granoblastic-eteroblastic	mainly straight (rare curved)	235±96	340±135	860	1047±431	0.073±0.056	284±110	290±111	728±76	831±75	697±123
	Fantiscritti	TO	granoblastic-eteroblastic	from curved to straight	212±91	303±127	730	929±415	0.058±0.048	253±106	258±108	748±82	839±75	709±124
Torano	La Facciata	LF	from xenoblasic to granoblastic-eteroblastic	from lobates to curved	188±70	271±94	600	827±314	0.044±0.031	224±77	228±79	751±83	836±82	707±134

Max and min: maximum and minimum crystal axes (μm); MGS: maximum grain size (μm); A: average grains area (μm^2); P: average grains perimeter (μm); L and S: long and short axes length of grains (μm); D: average diameter (μm); D_{eq}: equivalent diameter (μm); F: form factor; S: sphericity; E: elongation.

Table 4: Physical Parameters ± Standard Deviations of Studied Marbles

Sample ID	G (g/cm^3)	γ_d (g/cm^3)	AC ($mgcm^{-2}\ t^{0.5}$)	IC_P (%)	IC_V (%)	P (%)	SI (%)
OL	2.718 (5)	2.708 (1)	0.071 ± 0.01	0.10±0.01	0.26±0.02	0.29±0.03	91±6
GR	2.719	2.705	0.141±0.033	0.16±0.02	0.42±0.06	0.45±0.06	95±2
CO	2.718	2.711	0.024±0.003	0.08±0.01	0.21±0.01	0.25±0.02	83±8
P2	2.717	2.709	0.032±0.008	0.08±0.01	0.23±0.01	0.25±0.02	91±4
PET	2.718	2.711	0.024±0.004	0.08±0.01	0.21±0.02	0.27±0.02	78±9
GI	2.718	2.706	0.042±0.011	0.13±0.03	0.36±0.07	0.43±0.11	85±10
CG	2.721	2.709	0.027±0.004	0.08±0.01	0.23±0.02	0.29±0.02	79±12
FS	2.72	2.705	0.086±0.023	0.12±0.01	0.32±0.04	0.37±0.05	86±8
TO	2.717	2.705	0.140±0.018	0.14±0.01	0.37±0.03	0.39±0.03	97±2
LF	2.718	2.71	0.020±0.005	0.07±0.01	0.18±0.02	0.20±0.02	89±7

G = real density (g/cm^3); γ_d = apparent density (g/cm^3); AC = capillary coefficient ($mg/cm^2t^{0.5}$); IC_P and IC_V = water absorption by total immersion (%; expressed in function of mass (P) or in volume (V)); P = porosity (%; in volume); SI = saturation index (%).

pore structure of the damaged marbles, informing us about the penetration of consolidants into surface and/or inner pores.

As regards ethyl-silicate, variation up to 80-90% suggests a meaningful penetration of the product even more than the surface. As far as nano-silica product, the registered variation in capillary absorption coefficient (~70-80%) might suggest a high efficacy of the product in consolidating marbles; however, data obtained from total immersion test clearly indicate that the product does not penetrate enough into pore structures, conditioning only the outwards porosity opened by thermal degrade (surface cracking, surface grain detachment, etc.). Finally, as concerns nano-lime

Table 5: Variation of Water Absorption Parameters before and after Thermal Stress Cycles

	AC	*ΔAC (mg cm−2 s−0.5)*				*IC*	*ΔIC (%)*			
Sample ID	***Fresh***	***20x105±5°C***	***20x105w±5°C***	***1x250±5°C***	***1x550±5°C***	***Fresh***	***20x105±5°C***	***20x105w±5°C***	***1x250±5°C***	***1x550±5°C***
OL	0.071±0.010	0.111±0.014	0.289±0.043	0.297±0.039	1.348±0.079	0.10±0.01	0.03±0.01	0.11±0.02	0.12±0.02	0.72±0.04
GR	0.141±0.033	0.059±0.009	0.238±0.006	0.379±0.009	1.573±0.092	0.16±0.02	0.02±0.01	0.08±0.01	0.13±0.01	0.79±0.04
CO	0.024±0.003	0.070±0.006	0.313±0.033	0.211±0.039	1.090±0.048	0.08±0.01	0.03±0.01	0.13±0.01	0.08±0.02	0.54±0.04
P2	0.032±0.008	0.036±0.010	0.300±0.008	0.143±0.024	1.207±0.023	0.08±0.01	0.02±0.01	0.14±0.01	0.07±0.01	0.62±0.01
PET	0.024±0.004	0.109±0.011	0.323±0.016	0.217±0.014	1.198±0.089	0.08±0.01	0.03±0.01	0.13±0.01	0.09±0.01	0.60±0.05
GI	0.042±0.011	0.169±0.049	0.373±0.008	0.366±0.043	1.611±0.071	0.13±0.03	0.03±0.01	0.14±0.01	0.12±0.01	0.79±0.04
CG	0.027±0.004	0.087±0.002	0.313±0.011	0.246±0.009	1.198±0.016	0.08±0.01	0.02±0.01	0.14±0.01	0.10±0.02	0.62±0.02
FS	0.086±0.023	0.123±0.005	0.321±0.011	0.288±0.019	1.374±0.090	0.12±0.01	0.02±0.01	0.12±0.01	0.10±0.01	0.72±0.04
TO	0.020±0.005	0.034±0.017	0.267±0.007	0.170±0.013	1.026±0.075	0.07±0.01	0.02±0.01	0.12±0.01	0.08±0.01	0.52±0.05
LF	0.140±0.018	0.047±0.015	0.229±0.013	0.267±0.016	1.487±0.027	0.14±0.01	0.02±0.01	0.09±0.01	0.09±0.01	0.77±0.01

Capillarity coefficient variation (*ΔAC*) and water by total immersion variation (*ΔIC)* in percentage (%).

Table 6: Variation of Porosity and Saturation Index before and after thermal Stress Cycles

	Porosity	*ΔP (%)*				*Saturation Index*	*ΔSI (%)*			
Sample ID	***Fresh***	***20x105±5°C***	***20x105w±5°C***	***1x250±5°C***	***1x550±5°C***	***Fresh***	***20x105±5°C***	***20x105w±5°C***	***1x250±5°C***	***1x550±5°C***
OL	0.29±0.03	0.06±0.02	0.16±0.05	0.23±0.10	1.88±0.12	90.84±5.51	9.22±2.85	32.95±16.64	23.4±8.79	7.37±3.98
GR	0.45±0.06	0.02±0.01	0.16±0.03	0.36±0.01	2.14±0.13	95.23±1.68	0.06±7.33	10.06±5	3.81±1.98	1.69±2.48
CO	0.25±0.02	0.05±0.02	0.27±0.01	0.22±0.02	1.42±0.08	82.65±8.30	11.34±10.99	22.53±4.28	13.73±5.90	15.36±6.57
P2	0.25±0.02	0.03±0.01	0.24±0.03	0.09±0.07	1.57±0.07	90.96±4.38	6.47±4.68	31.48±10.92	28.44±15.04	12.65±3.89
PET	0.27±0.02	0.09±0.04	0.24±0.03	0.22±0.02	1.56±0.13	78.28±8.62	4.07±6.71	35.77±6.27	13.58±2.24	21.65±5.39
GI	0.43±0.11	0.07±0.05	0.29±0.07	0.30±0.10	2.09±0.13	85.15±10.19	2.21±8.19	24.95±15.03	7.93±5.81	19.2±6.19
CG	0.29±0.02	0.05±0.03	0.25±0.03	0.26±0.03	1.66±0.04	79.45±11.49	3.68±8.6	39.2±3.74	12.49±1.73	15.35±13.71
FS	0.37±0.05	0.04±0.02	0.16±0.02	0.21±0.02	1.92±0.08	85.5±7.88	6.49±8.63	35.93±0.7	17.76±6.17	2.87±1.32
TO	0.39±0.03	0.02±0.02	0.06±0.04	0.16±0.02	1.95±0.04	88.48±6.62	12.38±4.22	33.01±13.24	9.51±4.45	6.30±3.74
LF	0.20±0.02	0.03±0.01	0.21±0.02	0.20±0.02	1.38±0.18	97.21±1.91	8.18±3.55	39.29±6.32	14.31±3.76	6.88±2.56

ΔP = porosity variation and *ΔSI* = saturation index variation in percentage (%).

Table 7: Average Variation of Water Absorption Parameters for Studied Marbles before and after the Treatments with the Three Tested Products (Nano-Lime, Nano-Silica and Ethyl-Silicate)

	Capillary Absorption Variation ΔAC%			*Total Immersion Variation ΔIC%*		
Thermal Cycles	***Albi 700***	***Nanorestore***	***NanoEstel***	***Albi 700***	***Nanorestore***	***NanoEstel***
20x105±5°C	90	20	71	87	6	18
20x105w±5°C	89	61	84	86	18	27
1x250±5°C	90	34	83	89	8	20
1x550±5°C	90	17	87	86	8	34

Capillarity coefficient variation (*ΔAC*) and water by total immersion variation (*ΔIC)* in percentage (%).

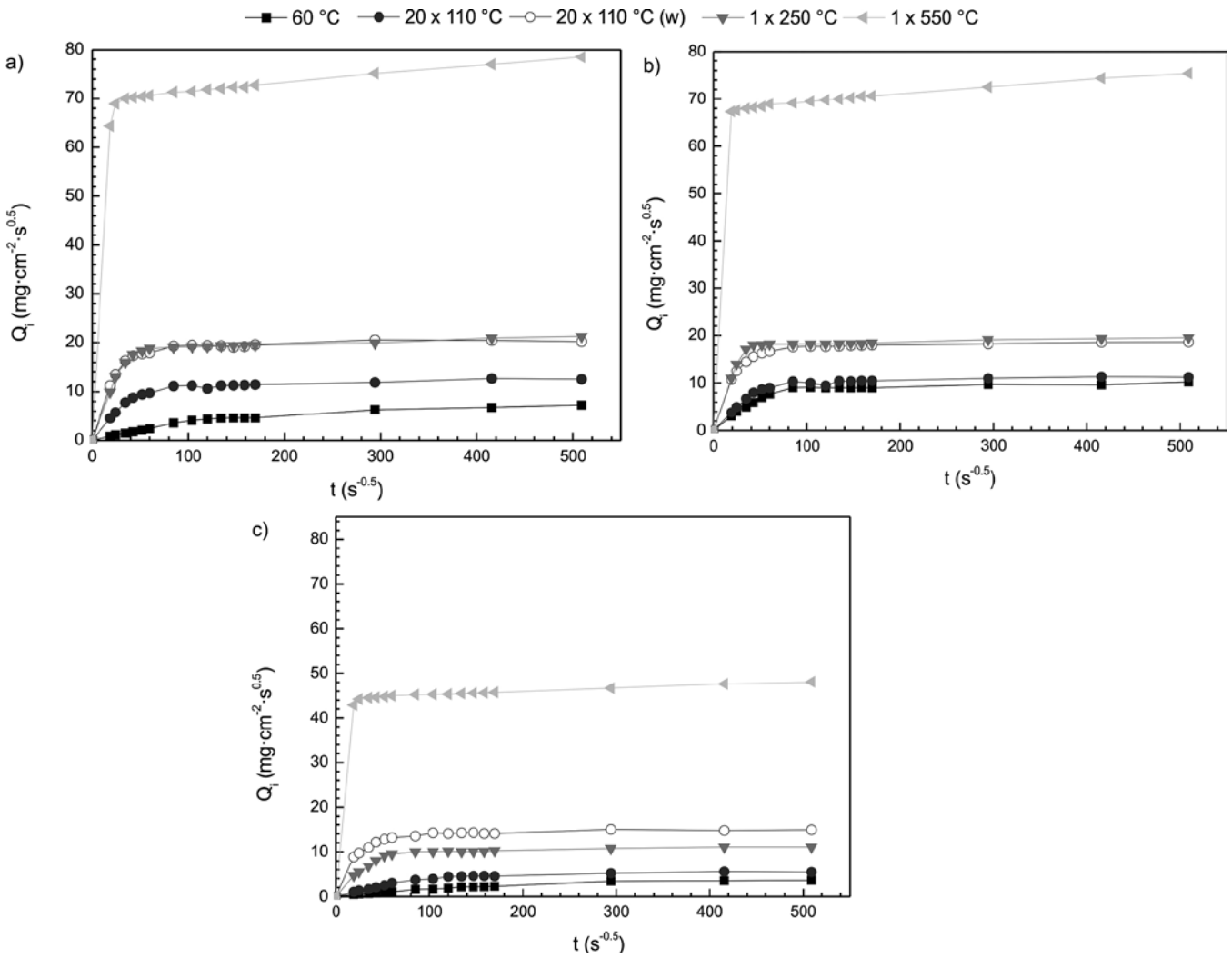

Figure 4: Capillarity absorption curves at different thermal stress cycles for (a) GI samples (straight boundaries), (b) TO samples (curved boundaries) and (c) LF samples (lobates boundaries), representative of marbles from Colonnata, Miseglia-Fantiscritti and Torano basins, respectively.

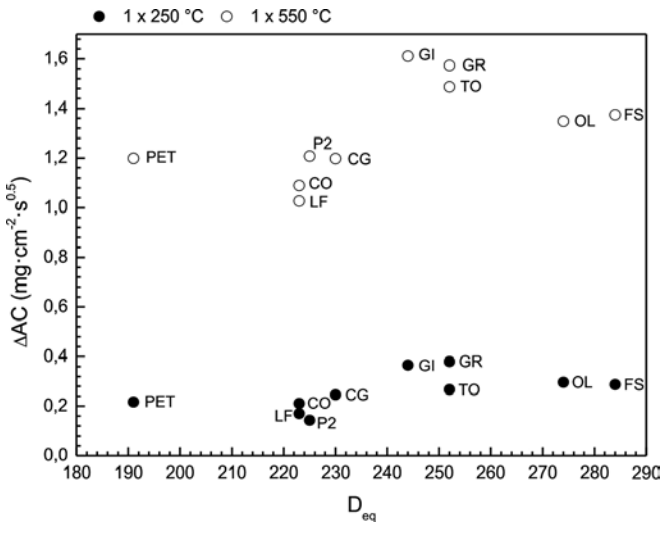

Figure 5: Variation of capillarity absorption coefficient (*ΔAC*) in function of grain size of analyzed marbles (expressed as D_{eq}). Comparison between values acquired on samples artificially damaged at 250°C and 550°C.

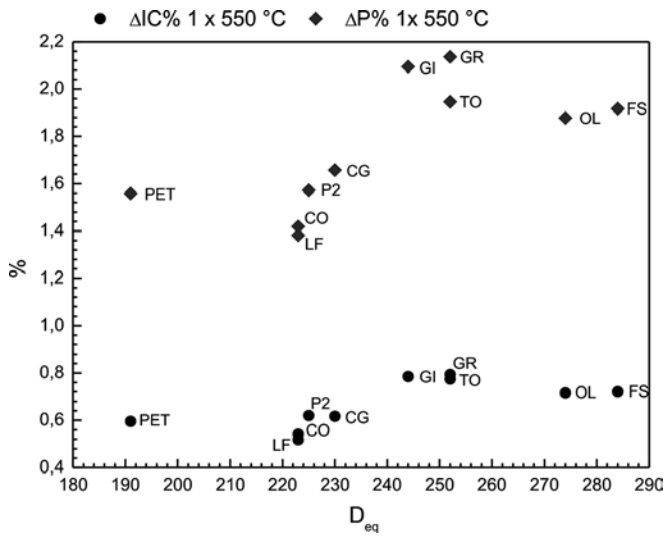

Figure 6: Variation of imbibition coefficient and porosity in function of grain size of studied marble (expressed as D_{eq}) referred to artificially damaged samples at 550°C.

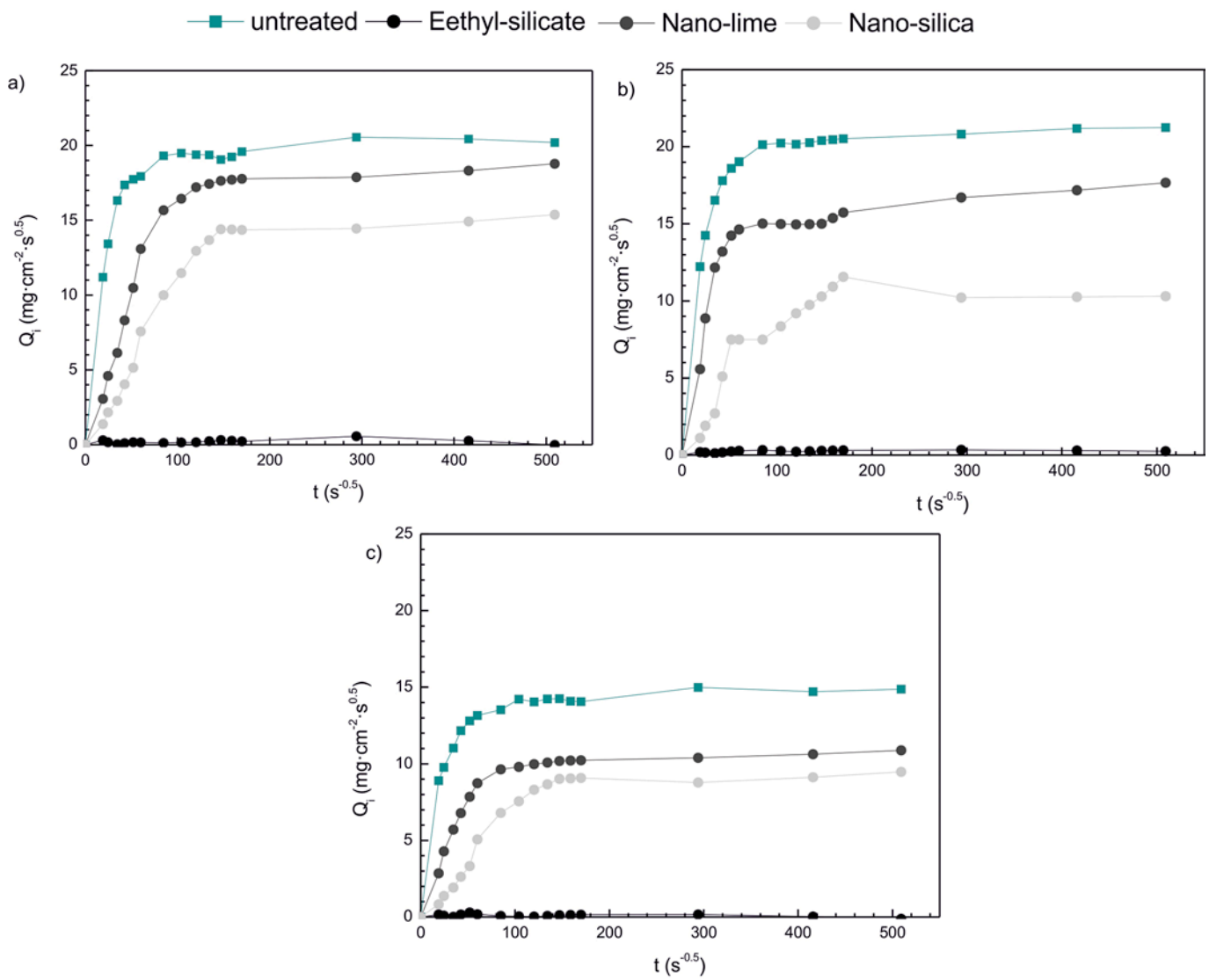

Figure 7: Variation of capillarity water absorption after treatment with ethyl-silicate, nano-lime and nano-silica for (a) GI samples (straight boundaries), (b) TO samples (curved boundaries) and (c) LF samples (lobates boundaries), as representative of marbles from Colonnata, Miseglia-Fantiscritti and Torano basins, respectively. Treated samples artificially damaged by 20 cycles at 105±5°C and cooled in water are shown, as example.

product, no relevant variations have been registered for both capillary and total immersion absorption. It is interesting to highlight that the higher variations of capillary absorption coefficient have been registered for marbles damaged at 105±5°C and cooled in water (ΔAC% ~ 60%). This behavior could be explained considering that thermal shock coupled with such a cooling determines the occurrence of intense degradation patterns close to the surface of marbles and the consequently opening of pores and cracks, the latter ones partially obstructed by nano-lime particles. However, the product is not able to penetrate over, as testified by the low variations in term of water absorbed by total immersion.

4. CONCLUSIONS

Despite the quite homogeneous composition, the ten marbles selected for this work showed a relevant range of textural features. Almost all marbles exhibited heteroblastic texture with grain boundaries from straight to curved, excepting for samples P2 (*Querciola* site, Carrara basin) and LF (*La Facciata* site, Torano basin) for which a xenoblastic texture with lobates grain boundaries was observed. The average grain size varied from 191 μm (minimum value measured for PET, Campanili site, Carrara basin) to 284 μm (maximum value for FS, Bocca Canalgrande, Miseglia-Fantiscritti basin), defining three groups with D_{eq}> 250 μm (FS and

OL), $D_{eq} \cong$ 250 µm (GI, GR e TO), and $D_{eq} <$ 250 µm (CG, CO, LF, P2 and PET).

Absorption tests evidenced that microfabric features affect the water behavior of marbles. In particular, an increasing of water absorption values (both by capillary and total immersion) along with grain size was observed; moreover, regardless grain size, marbles exhibiting straight and curves boundaries absorbed more water than marbles with lobates ones.

The already discussed texture variability influenced also the decay behavior of marbles. Marbles with grain size $\geq$ 250 µm and boundaries from straight to curved suffered a lot thermal damage than marbles with lower grain size and lobates grain boundaries. It is noteworthy that these trends are particularly evident after artificially thermal cycles up to 250°C.

Otherwise, texture did not affect the interaction between marbles and the tested consolidants. In fact, regardless grain size and grain boundaries: (i) ethyl-silicate efficaciously penetrates into pore structure of all studied marbles, assuring a great reduction of water absorption; (ii) nano-silica partially reduces the absorbed water, by penetrating only into surface porosity of marbles; (iii) nano-lime particles do not determines encouraging results, scarcely penetrating into pore structure and interesting mainly surface cracks induced by very intense decay (as in case of specimens thermally damaged at 105±5°C and cooled in water).

ACKNOWLEDGEMENTS

This work has been supported by the European program Horizon 2020 call NMP21-AC 646178, in the framework of the Nano-Cathedral project (Grant agreement 646178).

REFERENCES

[1] Molli G, Heilbronner R. Microstructures associated with static and dynamic recrystallization of Carrara Marble. (A.Apuane, NW Tuscany, Italy). Geol Mijnbouw 1999; 78: 119-126.
https://doi.org/10.1023/A:1003826904858

[2] Molli G, Conti P, Giorgetti G, Meccheri M, Oesterling N. Microfabric study on the deformational and thermal history of the Alpi Apuane marbles (Carrara marbles), Italy. J Struct Geol. 2000; 22: 1809-1825.
https://doi.org/10.1016/S0191-8141(00)00086-9

[3] Franzini M, Gratziu C, Spampinato M. Degradazione del marmo per effetto di variazioni di temperatura. Rend Soc It Miner Petrol. 1984; 39: 47-58.

[4] Franzini M. Stones in monuments: natural and anthropogenic deterioration of marble artifacts. Eur J Mineral. 1995; 7: 735-743.
https://doi.org/10.1127/ejm/7/4/0735

[5] Barsottelli M, Fratini F, Giorgetti G, Manganelli Del Fà C, Molli G. Microfabric and alteration in Carrara marble: a preliminary study. Sci Technol Cult Heritage 1998; 7: 115-126.

[6] Leiss B, Weiss T. Fabric anisotropy and its influence on physical weathering of different types of Carrara marbles. J Struct Geol. 2000; 22: 1737-1745.
https://doi.org/10.1016/S0191-8141(00)00080-8

[7] Siegesmund S, Ullemeyer K, Weiss T, Tschegg EK. Physical weathering of marbles caused by anisotropic thermal expansion. Int J Earth Sci. 2000; 89: 170-182.
https://doi.org/10.1007/s005310050324

[8] Vitaloni M, Lezzerini M. Marmi apuani e degrado termico: studio preliminare. In Atti del III Congresso Nazionale di Archeometria 2004; pp. 147-155.

[9] Cantisani E, Pecchioni E, Fratini F, Garzonio CA, Malesani P, Molli G. Thermal stress in the Apuan marbles: Relationship between microstructure and petrophysical characteristics. Int J Rock Mech Min Sc. 2009; 46: 129-137.
https://doi.org/10.1016/j.ijrmms.2008.06.005

[10] Delgado Rodrigues J, Grossi A. Indicators and ratings for the compatibility assessment of conservation actions. J Cult Heritage 2007; 8: 32-43.
https://doi.org/10.1016/j.culher.2006.04.007

[11] Doehne E, Price Clifford A. Stone Conservation. An Overview of Current Research. 2nd ed. The Getty Conservation Institute 2010.

[12] Baglioni P, Chelazzi D, Giorgi R. Nanotechnologies in the Conservation of Cultural Heritage. Firenze: Springer 2015.
https://doi.org/10.1007/978-94-017-9303-2

[13] Baglioni P, Giorgi R. Soft and hard nanomaterials for restoration and conservation of cultural heritage. Soft Matter 2006; 2: 293-303
https://doi.org/10.1039/b516442g

[14] Hansen E, Doehne E, Fidler J, Larson J, Martin B, Matteini M, *et al*. A review of selected inorganic consolidants and protective treatments for porous calcareous materials. Rev Conservat. 2003; 4:13-25.
https://doi.org/10.1179/sic.2003.48.supplement-1.13

[15] Gherardi F, Gulotta D, Goidanich S, Colombo A, Toniolo L. On-site monitoring of the performance of innovative treatments for marble conservation in architectural heritage. Heritage Science 2017; 5:4.
https://doi.org/10.1186/s40494-017-0118-5

[16] Russ JC. Practical stereology. New York and London: Plenum Press 1986.
https://doi.org/10.1007/978-1-4899-3533-5

[17] Lezzerini M, Tamponi M, Bertoli M. Reproducibility, precision and trueness of X-ray fluorescence data for mineralogical and/or petrographic purposes. Atti Soc Tosc Sci Nat Mem. Serie A 2013; 120: 67-73.

[18] Lezzerini M, Tamponi M, Bertoli M. Calibration of XRF data on silicate rocks using chemicals as in-house standards. Atti Soc Tosc Sci Nat Mem. Serie A 2014; 121: 65-70.

[19] Leone G, Leoni L, Sartori F. Revisione di un metodo gasometrico per la determinazione di calcite e dolomite. Atti Soc Tosc Sci Nat Mem. Serie A 1988; 95: 7-20.

[20] Hodgman C, Weast R, Selby S. Handbook of chemistry and physics; Cleveland: The Chemical Rubber publishing Co. 1961.

[21] Franzini M, Lezzerini M. A mercury-displacement method for stone bulk-density determinations. Eur J Mineral. 2003; 15: 225-229.
https://doi.org/10.1127/0935-1221/2003/0015-0225

[22] UNI EN 15801, 2010, Conservation of cultural property - test methods - determination of water absorption by capillarity.

[23] Weiss T, Siegesmund S, Fuller ERJ. Thermal degradation of marble: indications from finite-element modelling. Build Environ. 2003; 38: 1251-1260.
https://doi.org/10.1016/S0360-1323(03)00082-9

[24] UNI EN 14066, 2013, Natural Stone Test Methods - Determination of resistance to ageing by thermal shock.

[25] Koch A, Siegesmund S. The combined effect of moisture and temperature on the anomalous expansion behaviour of marble. Environl Geol. 2004; 46: 350-363.
https://doi.org/10.1007/s00254-004-1037-9

Received on 25-04-2017 Accepted on 23-05-2017 Published on 05-07-2017